RESEARCH PAPER

# Dopamine-conjugated apoferritin protein nanocage for the dual-targeting delivery of epirubicin

**Hasanain Gomhor J. Alqaraghuli [1, 2], Soheila Kashanian [3, 4*], Ronak Rafipour [5], Kamran Mansouri [6]**

[1]Department of Applied Chemistry, Faculty of Chemistry, Razi University, Kermanshah, Iran
[2]Department of Sciences, College of Basic Education, Al-Muthanna University, Al-Muthanna, Iraq
[3]Faculty of Chemistry, Sensor and Biosensor Research Center and Nanoscience and Nanotechnology Research Center, Razi University, Kermanshah, Iran
[4]Nano Drug Delivery Research Center, Kermanshah University of Medical Sciences, Kermanshah, Iran
[5]Department of Chemistry, Kermanshah Branch, Islamic Azad University, Kermanshah, Iran
[6]Medical Biology Research Center, Kermanshah University of Medical Sciences, Kermanshah, Iran

## ABSTRACT

***Objective(s):*** Nanocarriers are drug delivery vehicles, which have attracted the attention of researchers in recent years, particularly in cancer treatment. The encapsulation of anticancer drugs using protein nanocages is considered to be an optimal approach to reducing drug side-effects and increasing the bioavailability of anticancer drugs. Epirubicin (EPR) is an active chemotherapeutic medication used in the treatment of breast cancer. However, the toxicity of this drug against normal cells is a considerable limitation in therapy. EPR toxicity could be reduced using nanocarriers and dual-targeted drug delivery. Dual-targeted drug delivery system was developed by the conjugation of dopamine (DA) with horse spleen apoferritin (HsAFr)-encapsulated EPR to overcome the limitations of chemotherapeutic EPR in breast cancer treatment. HsAFr-EPR-DA complexes could target the scavenger receptors, transferrin receptors 1, and DA receptors, which are overexpressed on breast cancer cells.

***Materials and Methods:*** UV-Visible, fluorescence, and circular dichroism (CD) spectroscopic techniques and transmission electronic microscope (TEM) have been applied to characterize HsAFr-EPR-DA complexes. In the present study, we utilized human breast cancer cell line (MCF-7), aiming to compare the cytotoxicity of HsAFr-EPR-DA complexes to free EPR.

***Results:*** The toxicity was measured using the MTT assay, which demonstrated that the dual-targeted nanocarrier (HsAFr-EPR-DA) enhanced cytotoxicity against MCF-7 more significantly compared to non-targeted nanocarriers.

***Conclusion:*** The findings of the current research indicated that the synthesized HsAFr-DA complex was an optimal nanocarrier for the dual-targeted delivery of anticancer drugs.

***Keywords:*** *Dopamine, Drug Delivery, Dual Targeting, Epirubicin, Horse Spleen Apoferritin Nanocage*

**How to cite this article**

*J. Alqaraghuli HG, Kashanian S, Rafipour R, Mansouri K. Dopamine-conjugated apoferritin protein nanocage for the dual-targeting delivery of epirubicin. Nanomed J. 2019; 6(4): 250-257. DOI: 10.22038/nmj.2019.06.000002*

## INTRODUCTION

Breast cancer is the most prevalent cancer and the main cause of cancer deaths in women across the world. In 2012, reports estimated the number of cancer cases to be 1.7 million in women, with 522,000 deaths [1]. The treatments that are currently used for cancer therapy include surgery, chemotherapy, radiotherapy, immunotherapy, and targeted therapies. Nonetheless, the effectiveness of these strategies has been substantially impaired due to drug resistance mechanisms and their non-specific toxicity, prompting the development of new therapeutic strategies [2, 3]. Anthracyclines are anticancer chemotherapeutic agents, which are broadly utilized in the treatment of breast cancer. The anticancer activity of these drugs is through the inhibition of topoisomerase , which prevents DNA synthesis and leads to cell death [4, 5]. Recent studies have confirmed that anthracyclines increase the risk of clinical cardiotoxicity, thereby leading to heart failure [6]. Anthracyclines such

* *Corresponding Author Email: kashanian_s@yahoo.com*
Note. This manuscript was submitted on May 18, 2019; approved on August 5, 2019

as doxorubicin and epirubicin (EPR) are optical isomers, which are considered to be most active compared to other chemotherapeutic drugs [7]. Owing to its limited side-effects compared to doxorubicin, EPR is used for the treatment of breast cancer patients after the surgical removal of the tumor [8].Protein nanocages have been extensively investigated as drug delivery carriers in bionanotechnology [9]. These agents are considered to be potent nanocarriers owing to their biocompatible, nonimmunogenic, stability, and biodegradable nature [10].

Horse spleen apoferritin (HsAFr) is a spherical protein nanocage, which has been reported to be an effective nanocarrier for the dual-targeted drug delivery of cancer cells since it has more receptors on the membrane of cancer cells compared to normal cells. Furthermore, the surface of HsAFr contains numerous functional groups, which could be modified to prepare targeted ligands [11].

Ferritin is the protein involved in the storage of iron ions and is found in plants, animals, and humans. When iron ions are removed from the ferritin cavity, they are converted into apoferritin protein [12]. Each HsAFr is composed of 24 polypeptide subunits, which self-assemble to form a protein nanostructure [13]. In addition, HsAFr consists of two types of subunits, including the heavy and light chains, the molecular mass of which is 21,000 and 19,000 Da, respectively [14]. HsAFr has 14 channels that are located at the junctions of the protein subunits, among which eight threefold symmetric channels are hydrophilic, and six fourfold symmetric channels are hydrophobic [15]. HsAFr also contains a cage with the external diameter of 12 nanometers and inner cavity diameter of eight nanometers [16].

Encapsulation of anticancer drugs in HsAFr nanocages is based on pH-induced HsAFr dissociation and reassembly properties [17]. The subunits of HsAFr could be dissociated in strong acidic or alkaline environments (pH: 2 or 13) and associated by returning the pH to the physiological level (7.4) [18, 19]. HsAFr protein structure has been investigated at different pH levels by small angle X-ray scattering (SAXS) measurements. HsAFr is stable over a wide pH range (3.4-10), and denaturation of HsAFr occurs when it is heated at temperatures above 80°C for 10 minutes [20, 21].

In breast cancer cells, the cellular uptake of HsAFr nanocarriers occurs through the transferrin 1 receptor (TfR) and scavenger receptor, which are overexpressed in MCF-7 cells [22-24]. Moreover, the HsAFr surface could be modified with biomolecules such as antibodies [25], peptides [26], aptamers [27], and small molecules, such as dopamine [28].

In the advanced stages of the disease, breast cancer patients do not often respond to therapy, which urges the development of novel biomarkers and effective therapeutics. Dopamine (DA) receptors are found on breast cancer cells [29]; therefore, it is essential to target these receptors as the therapeutic targets in breast cancer [30]. DA is a biochemical substance with the formula of 3,4-dihydroxy-L-phenylalanine (catecholamine), which is secreted from the mussels [31]. DA receptors are a class of G-protein-coupled receptors. DA has five types of receptors, and it has been reported that dopamine type-1 receptor (D1R) is more significantly overexpressed in breast cancer cells than other cancer cell types [29].

The present study aimed to develop a dual-targeting delivery system for EPR anticancer drug using the HsAFr nanocage to reduce its side-effects on normal cells. In addition, DA was utilized as a targeting ligand. The proposed delivery system targets breast cancer cells via two receptors (TfR and DA receptors). In this article, cytotoxicity was estimated against the MCF-7 cell line in order to demonstrate the effectiveness of HsAFr-EPR-DA drug delivery system.

## MATERIALS AND METHODS

### *Experimental materials*

In this study, HsAFr was purchased from Callbiochem. Dopamine hydrochloride, 1-ethyl-3-(3-dimethylaminopropyl) carbodiimide (EDC) and *N*-hydroxysuccinimide (NHS) were purchased from Sigma-Aldrich, USA. Coomassie blue G-250 and 8-anilino-1-naphthalenesulfonate (ANS) were obtained from Merck, Germany. MCF-7 cells were purchased from the Pasteur Institute of Iran. EPR HCl was obtained from Ebewe Pharma, Austria. The other chemicals were obtained from Merck, Germany.

### *Synthesis of HsAFr-EPR-DA complexes*

The loading of EPR into HsAFr was achieved as described by H. Gomhor J. Alqaraghuli *et al.* [19], and the synthesis of HsAFr-EPR-DA complexes was carried out based on the modified methods proposed by Kim et al. and Lee et al. [32, 33].

EDC (0.5 mg) and NHS (0.3 mg) were dissolved

in one milliliter of phosphate buffer solution (pH: 6.6) for at the temperature of 25°C for 15 minutes in order to prepare the activation buffer. The activation buffer was added to one milligram of EPR-loaded HsAFr drop-wise with slow stirring. After 20 minutes, 0.2 milligram of DA was added, and the pH was adjusted to 6.8 using HCl (0.01 M), and the mixture was incubated for three hours. The solution was dialyzed against 0.01 M phosphate buffer solution (pH: 7.4, 450 ml) in triplicate at two-hour intervals so as to completely drive out the free DA molecules from the HsAFr-EPR-DA complexes.

***Characterization of the HsAFr-EPR-DA complexes***

The HsAFr-EPR-DA complexes were characterized using several techniques. Absorption spectra were performed using a UV-Vis spectrophotometer (model: Agilent 8453). The CD results were recorded using a spectropolarimeter (model JASCO J-810), and the transmission electronics microscopy (TEM) measurements were performed using a transmission electron microscope (Zeiss, model: EM10C-100 kV).

***Spectrofluorometric studies***

The fluorescence emission spectra were recorded using a quartz cuvette (path length: 1 cm) at the temperature of 25°C. The experiments for the fluorescence emission spectra were conducted using ANS by incubating the HsAFr protein solutions and 30 micrometers of ANS for 30 minutes. In addition, the fluorescence spectra were recorded at the excitation wavelength of 360 nanometers. It is notable that the samples without HsAFr were considered as controls.

***In-vitro study of EPR release from the HsAFr-DA nanocages***

The *in-vitro* study of EPR release from the HsAFr-DA nanocages was performed using the dialysis method. The HsAFr-EPR-DA sample was placed in a dialysis bag (cutoff: 12,000 Da). The dialysis bag was tied and immersed in 50 milliliters of 0.1 M phosphate buffer solution (pH: 7.4) at the temperature of 37°C, along with stirring at 120 rpm. At the time intervals of two, four, six, eight, 10, 12, 24, 36, 48, 60, 70, and 80 hours. Two milliliters of the aliquots of the release medium were removed, and the same volume of fresh phosphate buffer was added to the system. The amount of drug in the release medium was evaluated using the fluorescence technique based on the comparison to the standard curve; the EPR on the excitation of 482 nanometers indicated a strong fluorescence peak at 560 nanometers [34].

***Cell proliferation assays***

The effects of proliferation inhibition on the MCF-7 cancer cell line were determined using HsAFr-EPR-DA at the concentrations of 0.1, 0.2, 0.4, 0.8, 1.6, and 3.2 micrometers using the MTT assay. We used the MCF-7 obtained from the mammary gland and breast, which was a non-triple, negative human breast cell line. The cell line was seeded in 75-$cm^2$ tissue culture flasks and preserved in Dulbecco's MEM supplemented with 10% heat-inactivated fetal bovine serum, 100 U $mL^{-1}$ of penicillin, and 100 µg/$mL^{-1}$ of streptomycin. The medium was renewed every two days, and the cell cultures were incubated at the temperature of 37°C in a humid environment (95% air, 5% $CO_2$) [35, 36].

***TEM experiment***

The TEM experiment using HsAFr-EPR was achieved as described by H. Gomhor J. Alqaraghuli *et al*. [19].

***Stability of the HsAFr-EPR-DA complexes in storage***

The stability of the HsAFr-EPR-DA complexes was determined based on the modified method proposed by Kilic et al. [37]. The samples of the HsAFr-EPR-DA complex were preserved in phosphate buffer solution at the pH of 7.4 and temperature of 4°C and 37°C for six weeks. The released EPR molecules were removed from the samples every two weeks using a dialysis bag (cutoff: 12 KDa) using the diffusion technique with 50 milliliters of the same buffer for one hour. Following that, the HsAFr, EPR, and DA contents of the samples were determined using the Bradford assay and fluorescence technique.

**RESULTS AND DISSCUATION**

***Characterization of DA-conjugated EPR-loaded HsAFr***

HsAFr showed an absorption peak at 280 nm [38]. Absorption at 280 nanometers reflected the residues of the aromatic amino acid content in the HsAFr protein. On the other hand, the spectrum of red EPR showed the maxima at 481 nanometers [19, 39]. In addition, DA showed an absorption

band at 280 nanometers [40]. Absorption at 280 nanometers in DA was due to π→π* transition in the aromatic rings [41]. The UV-Vis spectra of the HsAFr-EPR-DA complexes were determined as well (Fig 1).

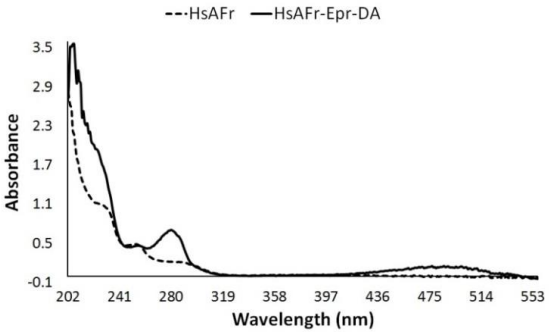


Fig 1. UV-Vis Spectra of HsAFr and HsAFr-EPR-DA Complexes Showing Absorbance Peaks at 280 and 481 nm

The UV-Vis spectra of the HsAFr-EPR-DA complexes were also verified in order to investigate the encapsulation of the drug in the apoferritin through the absorption observed at 481 nanometers, and the surface was modified HsAFr with DA through the absorption with high intensity at 280 nanometers. The number of the DA-targeting molecules was determined via UV-Vis spectrophotometry at 280 nanometers after using the blank HsAFr protein and EPR. The ratio of the HsAFr:DA molecules was 1:102. The DA fluorescence spectra in the DA solution and HsAFr-EPR-DA complexes were determined after using the blank HsAFr (Fig 2).

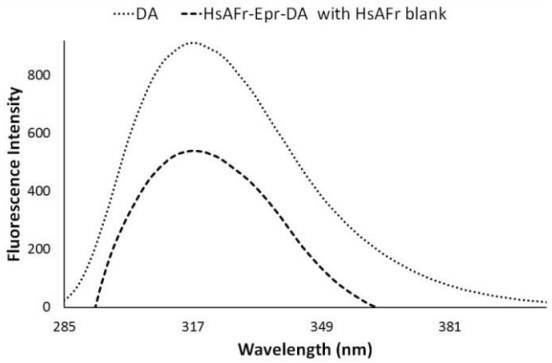


Fig2. Dopamine Fluorescence Spectra in DA Solution and HsAFr-EPR-DA Complexes (Excitation wavelength set at 279 nm; fluorescence spectra exhibited emission maximum at wavelength of 317 nm)

The DA fluorescence spectra were recorded at 285-405 nanometers at the excitation wavelength of 279 nanometers [42]. The HsAFr protein in the HsAFr-EPR-DA sample was measured using the Bradford assay to prepare the blank solution of HsAFr [43]. According to the findings, the fluorescence spectra of DA in the DA solution and HsAFr-Epr-DA complex exhibited an emission maximum at the wavelength of 317 nanometers. Moreover, the HsAFr surface was modified with DA in the HsAFr-EPR-DA complex.

***Effects of targeting and drug encapsulation on the HsAFr structure***

ANS is a fluorescent probe used to investigate conformational changes in proteins. ANS shows higher fluorescence intensity when binding to the hydrophobic sites of proteins [44, 45]. The hydrophobicity of drug carrier is an essential factor in this regard since it may affect the distribution, bioavailability, and solubility of the drug-carrier complex [46]. The fluorescence spectra of ANS, HsAFr-ANS, HsAFr-EPR-ANS, and HsAFr-EPR-DA-ANS demonstrated a maximum at the same wavelength (523 nm) for all HsAFr when they were all excited at 360 nanometers, with blue shifts in the wavelength (Fig 3).

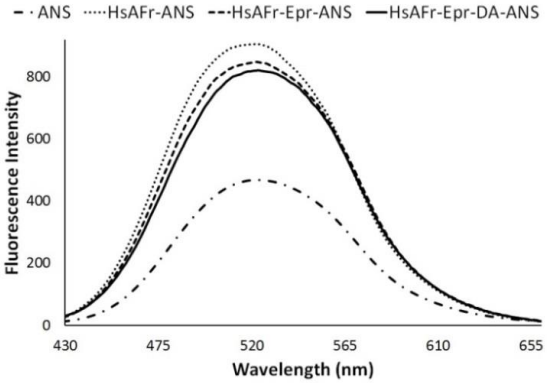


Fig 3. ANS Fluorescence Spectra of ANS, HsAFr-ANS, HsAFr-EPR-ANS, and HsAFr-EPR-DA-ANS (Excitation wavelength set at 360 nm; fluorescence spectra exhibited emission maximum at approximately same wavelength [523 nm])

ANS is weakly fluorescent in water, while its spectrum is blue-shifted, and its intensity significantly increased when binding to the proteinic nonpolar sites [47, 48]. In the present study, the ANS measurements were carried out to assess the occurrence of exposed hydrophobic surfaces in the HsAFr-EPR-DA complexes. No changes were observed in the fluorescence spectra of HsAFr after drug loading and DA targeting. Therefore, it could be concluded that the HsAFr protein was stable after drug loading and surface

modification with DA.In the current research, the far-UV CD spectra were recorded to investigate the changes in the secondary structure of HsAFr after surface modification with DA.Fig 4 depicts the CD spectra of the HsAFr-EPR-DA complexes and HsAFr within the range of 195-245 nanometers. HsAFr subunits are composed of α-helix bundles, which appeared in two clear negative peaks at 208 and 221 nanometers [49]. The CD spectra were still similar to the negative peaks, which indicated that the secondary structure in HsAFr remained almost constant before and after surface modification with DA. It is also notable that the CD spectra of HsAFr-EPR-DA reduced in terms of negative ellipticity, while indicating no changes in the secondary structure of apoferritin, which was still predominated by α-helix. In this regard, Jiang et al. and Liu et al. reported similar results in terms of apoferritin as a nanocarrier [19, 50, 51].

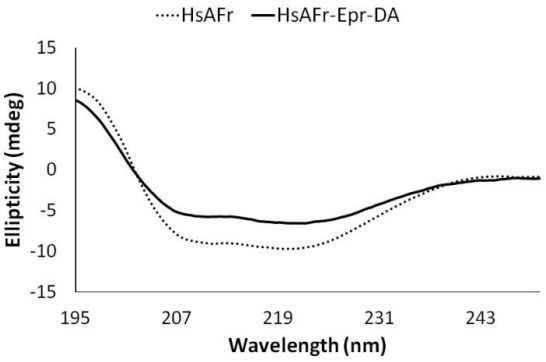


Fig 4. CD Spectra of HsAFr and HsAFr-EPR-DA Complexes (CD spectra exhibited two negative peaks at 208 and 221 nm)

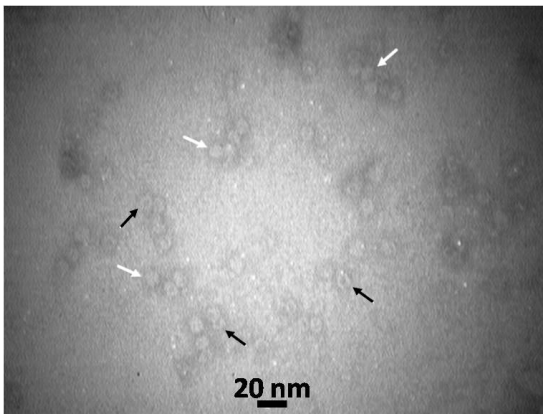


Fig 5. TEM Image of Negatively Stained EPR-loaded HsAFr (Presence and absence of EPR in cavity of HsAFr shown in white and black arrows)

***TEM***

Similar to the image presented in our previous study [19], Fig 5 shows the TEM result of the negatively stained, EPR-loaded HsAFr with uranyl acetate. When the EPR molecules were entrapped inside the HsAFr protein cages, the drug molecules prevented uranyl acetate from entering the inner cavity of HsAFr (white arrows). In case of HsAFr alone, uranyl acetate could enter the HsAFr cavity via channels after negative staining with uranyl acetate (black arrows) [52].

***In-vitro drug release from HsAFr-DA nanocages***

Fig 6 shows the EPR drug release profile from the HsAFr-DA nanocarriers in phosphate buffer in physiological conditions (pH: 7.4, 37°C) as a function of time. Moreover, the obtained results indicated the acceptable drug release at the pH of 7.4 to be approximately 25.34% of the loaded EPR that was released after eight hours, and 81.39% of the loaded EPR was released after 48 hours.

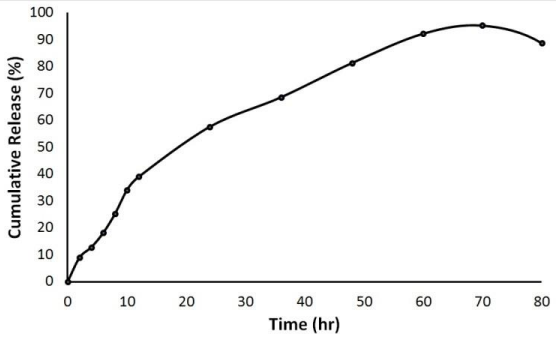


Fig 6. Rate of EPR Drug Release from HsAFr-DA Nanocarriers at pH of 7.4 (Release profiles of EPR in phosphate buffer solution at 37°C as function of time)

The inner surface of the HsAFr protein nanocage was rich in the acidic residues of glutamate (Glu) and aspartate (Asp) amino acids, resulting in a high negative charge density in the inner cavity of the HsAFr nanocage at physiological pH [53]. At the pH of 7.4, the carboxylic groups of Asp and Glu residues were ionized, and the drug molecules were neutral due to the non-protonation of its amino groups, which in turn led to the reduction of the electrostatic interaction of neutral EPR drug molecules with the negatively charged inner cavity of the apoferritin. This phenomenon led to drug release from EPR-loaded HsAFr-DA over time.

***In-vitro cytotoxicity of HsAFr-EPR-DA***

The cytotoxic activity of HsAFr, DA, EPR, HsAFr-DA, HsAFr-EPR and HsAFr-EPR-DA at various concentrations was assessed against the cultured MCF-7 cell lines using the MTT assay. After 24 hours, the $IC_{50}$ values of EPR, HsAFr-EPR, and

HsAFr-EPR-DA were estimated at 1.29, 0.54, and 0.32 µM, respectively. These findings suggested that the activity of HsAFr-EPR-DA against the MCF-7 cell line was more significant compared to HsAFr-EPR and free EPR.

Fig 7 shows the toxicity of HsAFr, DA, HsAFr-DA, EPR, HsAFr-EPR, and HsAFr-EPR-DA in the MCF-7 cell line. The MTT assay with 1.6 micrometers of EPR, EPR-loaded HsAFr, and HsAFr-EPR-DA reduced cell growth by 56%, 82.66%, and 100%, respectively. According to the obtained results, the toxicity of EPR-loaded HsAFr was higher compared to free EPR since HsAFr could enter the tumor cells through interactions with the scavenger receptor (CD163) and transferrin receptors 1 (TfR1) (CD71), which are overexpressed more significantly on the membrane of tumor cells [54-56]. The higher toxicity of HsAFr-EPR-DA suggested that the HsAFr nanocarriers have high affinity for tumor cells through the SCARA5 and TfR1 receptors via an endocytosis pathway. On the other hand, the presence of DA receptors on the membrane of breast cancer cells [57] indicated the dual-targeting delivery of EPR. Furthermore, the obtained data demonstrated no clear cytotoxicity at any of the concentrations of the synthesized HsAFr-DA, making it a safe and effective drug delivery carrier.

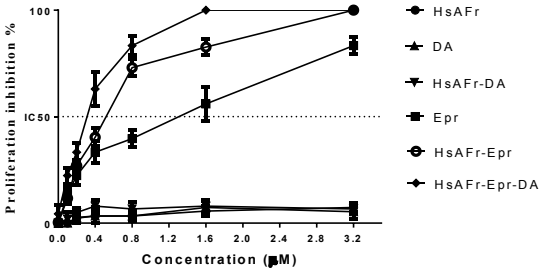


Fig 7. Proliferation Inhibition Effect of HsAFr-EPR-DA Compared to HsAFr, DA, HsAFr-DA, EPR, and HsAFr-EPR in MCF-7 Cell Line (IC50 values of EPR, HsAFr-EPR, and HsAFr-EPR-DA after 24 hours estimated at 1.29, 0.54, and 0.32 µM, respectively)

### *Stability of the HsAFr-EPR-DA complexes in storage*

The contents of the HsAFr-EPR-DA complex remained constant at the temperature of 4°C during six weeks indicated that the HsAFr shell was capable of holding the EPR molecules within the protein nanocage. The high stability of the drug-loaded HsAFr complexes seemed to be a general property of the highly stable structure of the HsAFr protein nanocage. In this regard, Dostalova et al. stated that doxorubicin within the HsAFr cage had no substantial changes for several weeks [37]. It is also notable that the high stability of the HsAFr-EPR-DA complex was a desirable property for its short-term storage as it could be preserved at the temperature of 4°C for several weeks as a drug delivery nanocarrier for therapeutic applications.

## CONCLUSION

In the present study, we developed a novel dual-targeted delivery system, and EPR as an anticancer drug was encapsulated in the core of the delivery system, which was composed of the HsAFr protein nanocage with DA utilized as a targeting ligand. Moreover, the ligand-based dual-targeted delivery system could be a new step toward the improvement of anticancer drugs to target cancer cells through a wide range of receptors. The HsAFr-EPR-DA complexes were successfully prepared, and their detailed characterization indicated that the HsAFr protein nanocage was stable after EPR loading and its surface modification with DA.

According to the findings regarding drug release, HsAFr provided a drug-controlled release from EPR-loaded HsAFr-DA, which was achieved at the pH of 7.4 and temperature of 37°C. The HsAFr-EPR-DA complex on the MCF-7 cell line was assessed, and the results indicated increased activity against the MCF-7 cell line compared to the free drug and HsAFr-EPR. Furthermore, the HsAFr-DA nanocarrier successfully delivered EPR and targeted breast cancer cells through the TfR and DA receptors. On the other hand, the obtained results demonstrated that dual-targeted nanocarriers could be utilized to target and improve the therapeutic efficacy of EPR as an anticancer drug. The HsAFr-EPR-DA sample was stable when preserved at the temperature of 4°C within six weeks. In conclusion, the findings of the current research implied that the synthesized HsAFr-DA complex was an optimal nanocarrier in the dual-targeted delivery of anticancer drugs.

## ACKNOWLEDGMENTS

The authors thank the Razi University Research Council for the support of this work.

## REFERENCES

1.Torre LA, Bray F, Siegel RL, Ferlay J, Lortet-Tieulent J, Jemal A. Global cancer statistics, 2012. CA Cancer J Clin. 2015; 65(2): 87-108.

2.Pais-Silva C, de Melo-Diogo D, Correia IJ. IR780-loaded TPGS-TOS micelles for breast cancer photodynamic therapy. Eur J Pharm Biopharm. 2017; 113: 108-117.

3.Miller KD, Siegel RL, Lin CC, Mariotto AB, Kramer JL, Rowland JH. Cancer treatment and survivorship statistics, 2016. CA Cancer J Clin. 2016; 66(4): 271-289.

4.Zagar TM, Cardinale DM, Marks LB. Breast cancer therapy-associated cardiovascular disease. Nat Rev Clin Oncol. 2016; 13(3): 172.
5.Mordente A, Meucci E, EttoreMartorana G, Tavian D, Silvestrini A. Topoisomerases and anthracyclines: recent advances and perspectives in anticancer therapy and prevention of cardiotoxicity. Curr Med Chem. 2017; 24(15): 1607-1626.
6.Perrino C, G Schiattarella G, Magliulo F, Ilardi F, Carotenuto G, Gargiulo G, et al. Cardiac side effects of chemotherapy: state of art and strategies for a correct management. Curr Vasc Pharmacol. 201412(1):106-16..
7.Netíková IRŠ, Slušná M, Tolasz J, Šťastný M, Popelka Š, Štengl V. A new possible way of anthracycline cytostatics decontamination. New J Chem. 2017; 41(10): 3975-3985.
8.Karimi F, Shojaei AF, Tabatabaeian K, Shakeri S. CoFe2O4 nanoparticle/ionic liquid modified carbon paste electrode as an amplified sensor for epirubicin analysis as an anticancer drug. J Mol Liq. 2017; 242: 685-689.
9.Rother M, Nussbaumer MG, Renggli K, Bruns N. Protein cages and synthetic polymers: a fruitful symbiosis for drug delivery applications, bionanotechnology and materials science. Chem Soc Rev. 2016; 45(22): 6213-6249.
10.Lee EJ, Lee NK, Kim I-S. Bioengineered protein-based nanocage for drug delivery. Adv Drug Deliv Rev. 2016; 106: 157-171.
11.Zangabad PS, Karimi M, Mehdizadeh F, Malekzad H, Ghasemi A, Bahrami S, et al. Nanocaged platforms: modification, drug delivery and nanotoxicity. Opening synthetic cages to release the tiger. Nanoscale. 2017; 9(4): 1356-1392.
12.Zang J, Chen H, Zhao G, Wang F, Ren F. Ferritin cage for encapsulation and delivery of bioactive nutrients: From structure, property to applications. Crit Rev Food Sci Nutr. 2017; 57(17): 3673-3683.
13.Zhen Z, Tang W, Chen H, Lin X, Todd T, Wang G, et al. RGD-modified apoferritin nanoparticles for efficient drug delivery to tumors. ACS nano. 2013; 7(6): 4830-4837.
14.Mosca L, Falvo E, Ceci P, Poser E, Genovese I, Guarguaglini G. Use of Ferritin-Based Metal-Encapsulated Nanocarriers as Anticancer Agents. Applied Sciences. 2017; 7(1): 101.
15.Wei J, Li YL, Gao PC, Lu Q, Wang ZF, Zhou JJ, et al. Assembling gold nanoparticles into flower-like structures by complementary base pairing of DNA molecules with mediation by apoferritins. Chem Commun (Camb). 2017; 53(33): 4581-4584.
16.Jang JS, Choi SJ, Kim SJ, Hakim M, Kim ID. Rational Design of highly porous SnO2 nanotubes functionalized with biomimetic nanocatalysts for direct observation of simulated diabetes. Adv Funct Mater. 2016; 26(26): 4740-4748.
17.Zhang S, Zang J, Chen H, Li M, Xu C, Zhao G. The size flexibility of ferritin nanocage opens a new way to prepare nanomaterials. Small. 2017; 13(37): 1701045.
18.Pontillo N, Ferraro G, Helliwell JR, Amoresano A, Merlino A. X-ray Structure of the Carboplatin-Loaded Apo-Ferritin Nanocage. ACS Med Chem Lett. 2017; 8(4): 433-437.
19.Gomhor JAH, Kashanian S, Rafipour R, Mahdavian E, Mansouri K. Development and characterization of folic acid-functionalized apoferritin as a delivery vehicle for epirubicin against MCF-7 breast cancer cells. Artif Cells Nanomed Biotechnol. 2018; 46(sup3): S847-s854.
20.Dostalova S, Heger Z, Kudr J, Vaculovicova M, Adam V, Stiborova M, et al. Apoferritin: protein nanocarrier for targeted delivery. Nano Based Drug Delivery Zagerb: IAPC Publishing. 2015: 217-33.
21.Kim M, Rho Y, Jin KS, Ahn B, Jung S, Kim H. pH-dependent structures of ferritin and apoferritin in solution: disassembly and reassembly. Biomacromolecules. 2011; 12(5): 1629-1640.
22.Dostalova S, Polanska H, Svobodova M, Balvan J, Krystofova O, Haddad Y. Prostate-Specific Membrane Antigen-Targeted Site-Directed Antibody-Conjugated Apoferritin Nanovehicle Favorably Influences In Vivo Side Effects of Doxorubicin. Sci Rep. 2018; 8(1): 8867.
23.Roy K, Patel YS, Kanwar RK, Rajkhowa R, Wang X, Kanwar JR. Biodegradable Eri silk nanoparticles as a delivery vehicle for bovine lactoferrin against MDA-MB-231 and MCF-7 breast cancer cells. Int J Nanomedicine. 2016; 11:25.
24.Danilo C, Gutierrez-Pajares JL, Mainieri MA, Mercier I, Lisanti MP, Frank PG. Scavenger receptor class B type I regulates cellular cholesterol metabolism and cell signaling associated with breast cancer development. Breast Cancer Res. 2013; 15(5): R87.
25.Dostalova S, Cerna T, Hynek D, Koudelkova Z, Vaculovic T, Kopel P. Site-directed conjugation of antibodies to apoferritin nanocarrier for targeted drug delivery to prostate cancer cells. ACS Appl Mater Interfaces. 2016; 8(23): 14430-14441.
26.Kitagawa T, Kosuge H, Uchida M, Iida Y, Dalman RL, Douglas T. RGD targeting of human ferritin iron oxide nanoparticles enhances in vivo MRI of vascular inflammation and angiogenesis in experimental carotid disease and abdominal aortic aneurysm. J Magn Reson Imaging. 2017; 45(4): 1144-1153.
27.Zhao J, Liu M, Zhang Y, Li H, Lin Y, Yao S. Apoferritin protein nanoparticles dually labeled with aptamer and horseradish peroxidase as a sensing probe for thrombin detection. Anal Chim Acta. 2013; 759: 53-60.
28.Le TH, Kim JH, Park SJ. Fabrication of CdTe quantum dots–apoferritin arrays for detection of dopamine. J Cryst Growth. 2017; 468: 788-791.
29.Borcherding DC, Tong W, Hugo ER, Barnard DF, Fox S, LaSance K. Expression and therapeutic targeting of dopamine receptor-1 (D1R) in breast cancer. Oncogene. 2016; 35(24): 3103.
30.Yin T, He S, Shen G, Ye T, Guo F, Wang Y. Dopamine receptor antagonist thioridazine inhibits tumor growth in a murine breast cancer model. Mol Med Rep. 2015; 12(3): 4103-4108.
31.Wu M, Zhang D, Zeng Y, Wu L, Liu X, Liu J. Nanocluster of superparamagnetic iron oxide nanoparticles coated with poly (dopamine) for magnetic field-targeting, highly sensitive MRI and photothermal cancer therapy. Nanotechnology. 2015; 26(11): 115102.
32.Kim S, Jang Y, Jang LK, Sunwoo SH, Kim T-i, Cho S-W. Electrochemical deposition of dopamine–hyaluronic acid conjugates for anti-biofouling bioelectrodes. J Mater Chem B2017;5(23):4507-. 13.
33.Lee D-W, Yun Y-P, Park K, Kim SE. Gentamicin and bone morphogenic protein-2 (BMP-2)-delivering heparinized-titanium implant with enhanced antibacterial activity and osteointegration. Bone. 2012; 50(4): 974-982.
34.Motiei M, Kashanian S. Preparation of amphiphilic chitosan nanoparticles for controlled release of hydrophobic drugs. J Nanosci Nanotechnol. 2017; 17(8): 5226-5232.
35.Vantangoli MM, Madnick SJ, Huse SM, Weston P, Boekelheide

K. MCF-7 Human Breast Cancer Cells Form Differentiated Microtissues in Scaffold-Free Hydrogels. PloS one. 2015; 10(8): e0135426-e.
36.Shadkam M, Mansouri K. DNA binding and cytotoxicity studies of magnetic nanofluid containing antiviral drug oseltamivir AU - Shahabadi, Nahid. J Biomol Struct Dyn. 2018: 1-9.
37.Kilic MA, Ozlu E, Calis S. A novel protein-based anticancer drug encapsulating nanosphere: Apoferritin-doxorubicin complex. J Biomed Nanotechnol. 2012; 8(3): 508-514.
38.Luo Y, Wang X, Du D, Lin Y. Hyaluronic acid-conjugated apoferritin nanocages for lung cancer targeted drug delivery. Biomater Sci. 2015; 3(10): 1386-1394.
39.Zalewski P, Firlej A, Medenecka B, Jankowska J, Mielcarek J, Oszczapowicz I. The use of UV-VIS spectroscopy for determining the photostability of epirubicin solutions2009. 43-8 p.
40.Hayat A, Andreescu D, Bulbul G, Andreescu S. Redox reactivity of cerium oxide nanoparticles against dopamine. J Colloid Interface Sci. 2014; 418: 240-245.
41.Barreto W, Ponzoni S, Sassi P. A Raman and UV-Vis study of catecholamines oxidized with Mn (III). Spectrochimica Acta Part A: Molecular and Biomolecular Spectroscopy. 1998; 55(1): 65-72.
42.Fonseca BM, Rodrigues M, Cristóvão AC, Gonçalves D, Fortuna A, Bernardino L, et al. Determination of catecholamines and endogenous related compounds in rat brain tissue exploring their native fluorescence and liquid chromatography. J Chromatogr B. 2017; 1049 :51-59.
43.Chang SK, Zhang Y. Protein analysis. Food analysis: Springer; 2017. p. 315-31.
44.Satish L, Millan S, Bera K, Mohapatra S, Sahoo H. A spectroscopic and molecular dynamics simulation approach towards the stabilizing effect of ammonium-based ionic liquids on bovine serum albumin. New J Chem. 2017; 41(19): 10712-10722.
45.Matsumiya K, Suzuki YA, Hirata Y, Nambu Y, Matsumura Y. Protein–surfactant interactions between bovine lactoferrin and sophorolipids under neutral and acidic conditions. Biochem Cell Biol. 2017; 95(1): 126-132.
46.Jafari M, Karunaratne DN, Sweeting CM, Chen P. Modification of a designed amphipathic cell-penetrating peptide and its effect on solubility, secondary structure, and uptake efficiency. Biochemistry. 2013; 52(20): 3428-3435.
47.Kashanian S, Tarighat FA, Rafipour R, Abbasi-Tarighat M. Biomimetic synthesis and characterization of cobalt nanoparticles using apoferritin, and investigation of direct electron transfer of Co (NPs)–ferritin at modified glassy carbon electrode to design a novel nanobiosensor. Molecular biology reports. 2012; 39(9): 8793-8802.
48.Ito D, Itagaki H. Clarification of the inner microenvironments in poly (N-isopropylacrylamide) hydrogels in macrogel and microgel forms using a fluorescent probe technique. Eur Polym J. 2018; 99: 277-283.
49.Ji X-T, Huang L, Huang H-Q. Construction of nanometer cisplatin core-ferritin (NCC-F) and proteomic analysis of gastric cancer cell apoptosis induced with cisplatin released from the NCC-F. J Proteom. 2012; 75(11): 3145-3157.
50.Liu X, Wei W, Wang C, Yue H, Ma D, Zhu C, et al. Apoferritin-camouflaged Pt nanoparticles: surface effects on cellular uptake and cytotoxicity. J Mater Chem A. 2011; 21(20): 7105-7110.
51.Jiang Y, Pang X, Wang X, Leung AW, Luan Y, Zhao G, et al. Preparation of hypocrellin B nanocages in self-assembled apoferritin for enhanced intracellular uptake and photodynamic activity. J Mater Chem B. 2017; 5(10): 1980-1987.
52.Lin C-Y, Yang S-J, Peng C-L, Shieh M-J. Panitumumab-Conjugated and Platinum-cored pH-sensitive Apoferritin Nanocages for Colorectal Cancer-targeted Therapy. ACS Appl Mater Interfaces. 2018; 10(7): 6096-6106.
53.Zhang S, Zang J, Chen H, Li M, Xu C, Zhao G. The Size Flexibility of Ferritin Nanocage Opens a New Way to Prepare Nanomaterials. Small. 2017; 13(37).
54.Belletti D, Pederzoli F, Forni F, Vandelli MA. Protein cage nanostructure as drug delivery system: magnifying glass on apoferritin. 2017; 14(7): 825-840.
55.Conti L, Lanzardo S, Ruiu R, Cadenazzi M, Cavallo F, Aime Sl. L-Ferritin targets breast cancer stem cells and delivers therapeutic and imaging agents. Oncotarget. 2016; 7(41): 66713-66727.
56.Aleksandrowicz R, Taciak B, Krol M. Drug delivery systems improving chemical and physical properties of anticancer drugs currently investigated for treatment of solid tumors. J Physiol Pharmacol. 2017; 68(2): 165-174.
57.Li J, Yao Q-y, Xue J-s, Wang L-j, Yuan Y, Tian X-y, et al. Dopamine D2 receptor antagonist sulpiride enhances dexamethasone responses in the treatment of drug-resistant and metastatic breast cancer. Acta Pharmacol Sin. 2017; 38(9): 1282.